

# Localization of coherent signals without source number knowledge in unknown spatially correlated Gaussian noise <sup>☆</sup>

Cheng Qian <sup>a</sup>, Lei Huang <sup>a,\*</sup>, Yuhang Xiao <sup>a</sup>, H.C. So <sup>b</sup>

<sup>a</sup> Department of Electronic and Information Engineering, Shenzhen Graduate School, Harbin Institute of Technology, Shenzhen, China

<sup>b</sup> Department of Electronic Engineering, City University of Hong Kong, Hong Kong

## ARTICLE INFO

### Article history:

Received 9 June 2014

Received in revised form

1 November 2014

Accepted 6 December 2014

Available online 15 December 2014

### Keywords:

Direction-of-arrival (DOA) estimation

Fourth-order cumulant

Coherent signals

Joint diagonalization

Toeplitz matrix

## ABSTRACT

A new direction-of-arrival estimator for coherent signals in spatially correlated noise is devised in this paper. By constructing a set of fourth-order cumulant based Toeplitz matrices, the coherent signals can be decorrelated. Moreover, by utilizing the joint diagonalization structure of these Toeplitz matrices, a new cost function that does not require any *a priori* information of the source number is developed. Numerical examples are provided to demonstrate the effectiveness of the proposed approach.

© 2015 Elsevier B.V. All rights reserved.

## 1. Introduction

Direction finding using a sensor array is an important task in many applications, such as radar [1], sonar [2] and wireless communications [3]. Numerous direction-of-arrival (DOA) estimators have been proposed in the literature. Among them, subspace based DOA estimation methods, such as ESPRIT [4–6] and MUSIC [7–9], provide an excellent solution to this problem when the following three assumptions are satisfied:

**A1** The number of sources is known *a priori*.

**A2** The sources are mutually uncorrelated or partially correlated.

**A3** The noise is spatially uncorrelated white noise, i.e., the covariance matrix is proportional to the identity matrix.

If any one of the above assumptions does not hold, this kind of techniques may suffer serious performance degradation.

As a matter of fact, the source number is usually unknown to the receiver in practice. To circumvent this issue, various source enumeration approaches have been suggested. Akaike information criterion (AIC) [10,11] and minimum description length (MDL) [12–15] are the most popular methods to estimate the number of sources. However, when the sample size is small and the signal-to-noise ratio (SNR) is low, they might not provide correct estimate of the source number. Although numerous modified algorithms have been proposed, the correct detection probability is still low in extreme conditions, especially when the noise property is unknown [13].

The **A2** cannot be satisfied in practice due to multipath propagation, which leads to many coherent components

<sup>☆</sup> The work described in this paper was in part supported by the NSFC/RGC Joint Research Scheme sponsored by the Research Grants Council of Hong Kong and the National Natural Science Foundation of China (Project No.: N-CityU 104/11, 61110229/61161160564), by the National Natural Science under Grant 61222106 and Grant 61171187 and by the Shenzhen Kongqie Talent Program under Grant YFZZ20111013.

\* Corresponding author.

E-mail addresses: [chengqian@hitsz.edu.cn](mailto:chengqian@hitsz.edu.cn) (C. Qian), [dr.lei.huang@ieee.org](mailto:dr.lei.huang@ieee.org) (L. Huang), [yuhangxiao@outlook.com](mailto:yuhangxiao@outlook.com) (Y. Xiao), [hcs0@ee.cityu.edu.hk](mailto:hcs0@ee.cityu.edu.hk) (H.C. So).

among the received data. Under such a case, the source covariance matrix is rank deficient, which in turn makes subspace based techniques to suffer serious performance degradation. Spatial smoothing (SS) technique and its variants [16–18] have been proposed to handle the coherent signals. They use a preprocessing scheme that first partitions the total array into subarrays and then averages the subarray output covariance matrices to make the source covariance matrix to be full rank, enabling the subspace based algorithms to work properly.

It is well known that most of the DOA estimation techniques are sensitive to the noise model [19,20] because they implicitly assume spatially uncorrelated noise. The spatially correlated noise can be easily handled by pre-whitening [21] provided that its covariance matrix is known *a priori*. However, in practice, since the array response and noise covariance are often computed from limited observations, an accurate covariance structure is often not available. The technique suggested in [22] is based on a parametric model to determine the noise covariance matrix, which allows the signal and noise parameters to be estimated simultaneously. In [23], a maximum likelihood (ML) based DOA estimation method has been proposed. It uses a set of sparse sensor arrays with multiple widely separated subarrays to make sensor noise uncorrelated between different subarrays, and then applies the ML method to estimate the DOAs.

The conventional array processing techniques are usually based on the covariance matrix which corresponds to the second-order statistics of the received signals. Indeed, the received signals are often non-Gaussian in practice, e.g., the BPSK, QPSK and QAM modulated signals. For non-Gaussian signals, the second-order statistics are not sufficient to characterize their statistical behavior. Higher-order moments are preferred to explore the non-Gaussianity of the signals. A number of higher-order statistics based DOA estimators have been proposed in the literature. Zeng et al. [24] use a set of fourth-order cumulant matrices to devise a new DOA estimation method that does not need to know the source number. However, it cannot deal with the coherent signals. Doğan and Mendel [25] use the higher-order cumulant to generate virtual aperture and then devise a virtual-ESPRIT algorithm (VESPA) which utilizes the information between virtual and actual sensors to solve the problem of joint array calibration and DOA estimation. The VESPA works properly for uncorrelated signals. For coherent signals, an extended VESPA (EVESPA) [26] has been proposed. Since each signal eigenvector associated with a group of coherent signals contains all the DOA information of these signals, the EVESPA applies the SS technique to this signal eigenvector to construct a full-rank signal subspace. Then it utilizes the root-MUSIC method to yield the DOA estimates. In [27], a higher-order cumulant MUSIC algorithm has been developed. This scheme can correctly work for the underdetermined case where the number of signals is larger than the number of sensors, but it is unable to handle the coherent signals.

To overcome the aforementioned shortcomings of the existing subspace based DOA estimators, we propose a new DOA estimator that is based on the joint diagonalization of a set of Toeplitz matrices. In this paper, we consider a

centro-symmetric uniform linear array (ULA) of  $N = 2M + 1$  sensors with half-wavelength interelement spacing. By employing the fourth-order cumulant technique, the Gaussian noise can be eliminated. Moreover,  $(2M + 1)(M + 1)$  different cumulant matrices can be formed, allowing us to handle the coherent signal issue. In particular, each row of a cumulant matrix is used to construct a Toeplitz matrix to decorrelate the coherent signals. Since these Toeplitz matrices share the joint diagonalization structure, a new cost function that does not need *a priori* information of source number is devised. A new spatial spectrum is then obtained where the DOAs are estimated via a *one-dimensional* search.

The remainder of the paper is organized as follows. Section 2 describes the direction finding problem and introduces the mathematical assumptions. The definition of the fourth-order cumulant, calculation of the Toeplitz covariance matrix and joint diagonalization based DOA estimation method are presented in Section 3. Simulation results are given in Section 4. Finally, conclusions are drawn in Section 5.

Throughout this paper, we use boldface uppercase letters to denote matrices, boldface lowercase letters for column vectors, and lowercase letters for scalar quantities. Superscripts  $(\cdot)^T$ ,  $(\cdot)^*$ ,  $(\cdot)^H$ ,  $(\cdot)^{-1}$  and  $(\cdot)^\dagger$  represent transpose, complex conjugate, conjugate transpose, inverse and pseudo-inverse, respectively. The operator  $\mathbb{E}\{a\}$  is the expected value of  $a$ ,  $\mathbf{0}$  is the zero matrix,  $\mathbf{I}_M$  is the  $M \times M$  identity matrix and  $\mathbf{J}_M$  is a  $M \times M$  exchanging matrix with its anti-diagonal being one and zero elsewhere. The  $\mathbb{C}$  denotes the set of complex numbers. Furthermore,  $\|\cdot\|$  represents the Euclidean norm of a vector.

## 2. Problem formulation

Consider a ULA with  $N = 2M + 1$  isotropic sensors shown in Fig. 1. There are  $P$  ( $P \leq M + 1$ ) narrowband source signals impinging on the array from distinct directions  $\{\theta_1, \dots, \theta_P\}$  in the far field and the first  $K$  signals are mutually coherent and the others are uncorrelated and independent of the first  $K$  signals. Taking the first signal  $s_1(t)$  as reference, the  $k$ th coherent signal becomes

$$s_k(t) = \beta_k e^{j\delta\phi_k} s_1(t), \quad k = 2, \dots, K \quad (1)$$

where  $\beta_k$  is the amplitude fading factor and  $\delta\phi_k$  is the phase change. Since the values of  $\delta\phi_k$  will not affect the coherence between the signals, without loss of generality, we set  $\delta\phi_k = 0, k = 2, \dots, K$ . Then the signals arriving at the  $m$ th sensor at time  $t$  can be expressed as

$$x_m(t) = \sum_{i=1}^P s_i(t) e^{-j2\pi m \sin(\theta_i)\Delta/\lambda} + n_m(t)$$

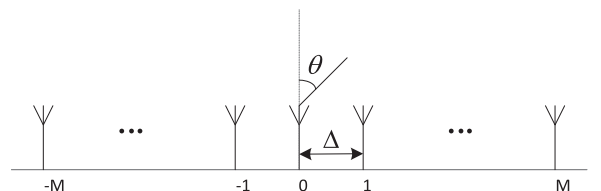


Fig. 1. Symmetric ULA model.

$$= s_1(t) \sum_{i=1}^K \beta_i e^{-j2\pi m \sin(\theta_i) \Delta / \lambda} + \sum_{i=K+1}^P s_i(t) e^{-j2\pi m \sin(\theta_i) \Delta / \lambda} + n_m(t) \quad (2)$$

where  $s_i(t)$  is the complex envelope of the  $i$ th signal,  $\beta_i = 1$ ,  $\lambda$  is the carrier wavelength,  $\Delta = \lambda/2$  is the interelement spacing. In vector form, (2) becomes

$$\mathbf{x}(t) = [x_{-M}(t), \dots, x_0(t), \dots, x_M(t)]^T = \mathbf{A}(\theta) \mathbf{s}(t) + \mathbf{n}(t) \quad (3)$$

where  $\mathbf{s}(t) = [s_1(t), \dots, s_P(t)]^T$  is the source signal vector and  $\mathbf{A} = [\mathbf{a}(\theta_1), \dots, \mathbf{a}(\theta_p)]$  is the array manifold with

$$\mathbf{a}(\theta_p) = [e^{j2\pi m \sin(\theta_p) \Delta / \lambda}, \dots, 1, \dots, e^{-j2\pi m \sin(\theta_p) \Delta / \lambda}]$$

being the  $p$ th steering vector. Here,  $\mathbf{n}(t)$  is assumed to be circularly symmetric zero-mean Gaussian with second-order moments such that [19,20]

$$\mathbb{E}[\mathbf{n}(t)] = \mathbf{0} \quad (4)$$

and

$$\mathbb{E}[\mathbf{n}(t_1) \mathbf{n}^H(t_2)] = \delta_{t_1, t_2} \mathbf{R}_n \quad (5)$$

$$\mathbb{E}[\mathbf{n}(t_1) \mathbf{n}^T(t_2)] = \mathbf{0} \quad (6)$$

where  $\mathbf{R}_n$  is a  $N \times N$  unknown positive definite Hermitian matrix representing the spatial correlation of noise, and  $\delta_{t_1, t_2}$  is Kronecker delta function which is defined as

$$\delta_{t_1, t_2} = \begin{cases} 0, & t_1 \neq t_2 \\ 1, & t_1 = t_2. \end{cases} \quad (7)$$

### 3. Proposed algorithm

#### 3.1. Fourth-order cumulant

Conventional array processing techniques utilize only the second-order statistics of data samples. The second-order statistics are sufficient provided that the signals are Gaussian distribution [25]. However, in most communication systems, we often prefer to use non-Gaussian signals, e.g., QAM and BPSK, for which the second-order statistics cannot completely characterize their statistical properties. Therefore, it is beneficial to consider the information embedded in higher-order statistics. In this section, we use the fourth-order cumulant matrix instead of the conventional sample covariance matrix (SCM) to eliminate the spatially colored Gaussian noise. The fourth-order cumulant of zero-mean stationary signals is defined as [27]

$$\begin{aligned} & \text{cum}(x_{k_1}(t), x_{k_2}^*(t), x_{l_1}(t), x_{l_2}^*(t)) \\ &= E\{x_{k_1}(t) x_{k_2}^*(t) x_{l_1}(t) x_{l_2}^*(t)\} \\ & - E\{x_{k_1}(t) x_{k_2}^*(t)\} E\{x_{l_1}(t) x_{l_2}^*(t)\} \\ & - E\{x_{k_1}(t) x_{l_1}(t)\} E\{x_{k_2}^*(t) x_{l_2}^*(t)\} \\ & - E\{x_{k_1}(t) x_{l_2}^*(t)\} E\{x_{k_2}^*(t) x_{l_1}(t)\} \end{aligned} \quad (8)$$

where  $-M \leq k_1, k_2, l_1, l_2 \leq M$ .

Define a  $M \times M$  cumulant matrix  $\mathbf{C}_{k_1, k_2}$  with its  $(l_1, l_2)$  entry being

$$\mathbf{C}_{k_1, k_2}(l_1, l_2) = \text{cum}(x_{k_1}(t), x_{k_2}^*(t), x_{l_1}(t), x_{l_2}^*(t)). \quad (9)$$

Collecting (9) for  $-M \leq l_1, l_2 \leq M$  in matrix form, we obtain

$$\mathbf{C}_{k_1, k_2} = \text{cum}(x_{k_1}(t), x_{k_2}^*(t), \mathbf{x}(t), \mathbf{x}^*(t)) = \mathbf{A}(\theta) \mathbf{\Gamma}_{k_1, k_2} \mathbf{A}^H(\theta) \quad (10)$$

where

$$\mathbf{\Gamma}_{k_1, k_2} \triangleq \begin{pmatrix} \gamma_{4, s_1} a_{l_1 1} a_{l_2 1}^* & & \\ & \ddots & \\ & & \gamma_{4, s_p} a_{l_1 p} a_{l_2 p}^* \end{pmatrix}. \quad (11)$$

Here,  $a_{mn} = e^{-j2\pi m \sin(\theta_n)/d}$  is the  $m$ th element of the  $n$ th steering vector and  $\gamma_{4, s_p} = \text{cum}(s_p(t), s_p^*(t), s_p(t), s_p^*(t))$  is the fourth-order cumulant of the  $p$ th source.

Since  $-M \leq l_1, l_2 \leq M$ , it is observed from (9) that we can construct  $(2M+1)^2$  cumulant matrices in total. However, due to the fact that  $\mathbf{C}_{k_1, k_2}$  is a centro-Hermitian matrix, we have

$$\mathbf{C}_{k_1, k_2} = \mathbf{C}_{k_2, k_1}^H \quad (12)$$

which means that  $\mathbf{C}_{k_1, k_2}$  and  $\mathbf{C}_{k_2, k_1}$  contain the same statistical information, i.e., they share the same eigenvectors and eigenvalues. Therefore, we do not need to compute all the  $(2M+1)^2$  cumulant matrices. Instead, we just need  $(2M+1)(M+1)$  cumulant matrices that have different statistics to be used for DOA estimation.

#### 3.2. Decorrelated procedure

Note that  $\mathbf{\Gamma}_{k_1, k_2}$  has full rank when all the signals are uncorrelated. However, when there exists highly correlated or even coherent sources,  $\mathbf{\Gamma}_{k_1, k_2}$  becomes rank deficient, which leads to performance degradation for conventional subspace based techniques. To circumvent this issue, a decorrelated procedure is required before DOA estimation.

**Proposition 1.** Given a fourth-order cumulant matrix  $\mathbf{C}_{k_1, k_2}$ , its  $(l_1, l_2)$  entry can be expressed as

$$\mathbf{C}_{k_1, k_2}(l_1, l_2) = \sum_{n=1}^P \phi_{k_1, k_2, l_1}(n) \cdot e^{j2\pi l_2 \sin(\theta_n)/d}. \quad (13)$$

where

$$\phi_{k_1, k_2, l_1}(n) = \begin{cases} \beta_n^* \gamma_{4, s_1} \sum_{p=1}^K \sum_{q=1}^K \sum_{m=1}^K a_{k_1 p} a_{k_2 q}^* a_{l_1 m} \beta_p \beta_q^* \beta_m, & n=1, \dots, K \\ \gamma_{4, s_n} \cdot |\beta_n|^4 a_{k_1 n} a_{k_2 n}^* a_{l_1 n}, & n=K+1, \dots, P \end{cases}$$

**Proof.** The proof is provided in Appendix A.

Given a cumulant matrix  $\mathbf{C}_{k_1, k_2}$ , similar to [28,31], by choosing its  $m$ th row, we can construct the following Toeplitz matrix:

$$\begin{aligned} \tilde{\mathbf{C}}_{k_1, k_2, m} &= \begin{bmatrix} c_{k_1, k_2}(m, 0) & c_{k_1, k_2}(m, 1) & \cdots & c_{k_1, k_2}(m, M) \\ c_{k_1, k_2}(m, -1) & c_{k_1, k_2}(m, 0) & \cdots & c_{k_1, k_2}(m, M-1) \\ \vdots & \vdots & \ddots & \vdots \\ c_{k_1, k_2}(m, -M) & c_{k_1, k_2}(m, -M+1) & \cdots & c_{k_1, k_2}(m, 0) \end{bmatrix} \\ &= \tilde{\mathbf{A}} \tilde{\mathbf{\Phi}}_{k_1, k_2, m} \tilde{\mathbf{A}}^H \in \mathbb{C}^{(M+1) \times (M+1)} \end{aligned} \quad (14)$$

where

$$\tilde{\mathbf{A}} = [\tilde{\mathbf{a}}(\theta_1), \dots, \tilde{\mathbf{a}}(\theta_P)] \quad (15)$$

$$\tilde{\Phi}_{k_1, k_2, m} = \begin{bmatrix} \phi_{k_1, k_2, m}(1) & & \\ & \ddots & \\ & & \phi_{k_1, k_2, m}(P) \end{bmatrix} \quad (16)$$

with

$$\tilde{\mathbf{a}}(\theta_p) = [1, e^{-j2\pi \sin(\theta_p)\Delta/\lambda}, \dots, e^{-j2\pi M \sin(\theta_p)\Delta/\lambda}]^T, \quad p = 1, \dots, P. \quad (17)$$

It is observed from (14) that  $\tilde{\mathbf{A}}$  is a Vandermonde matrix and the vectors  $\{\tilde{\mathbf{a}}(\theta_1), \dots, \tilde{\mathbf{a}}(\theta_P)\}$  are linearly independent. Therefore,  $\tilde{\mathbf{A}}$  is full column rank. Meanwhile, from Proposition 1 we find that  $\phi_{k_1, k_2, m}(p) \neq 0$  for  $p = 1, \dots, P$ . Thus,  $\tilde{\Phi}_{k_1, k_2, m}$  is a full rank diagonal matrix regardless of the coherence of sources.

**Remark 1.** Notice that any row of the fourth-order cumulant matrix can be used to form a Toeplitz matrix  $\tilde{\mathbf{C}}_m$ . In [28], an ESPRIT-like algorithm has been devised to utilize the SCM to form  $\mathbf{R}_m$ , and then the ESPRIT algorithm is employed for DOA estimation. However, it has three main demerits: (i) Every time it only uses one Toeplitz matrix to estimate the DOAs, which means that only partial information of the SCM is utilized. Hence, the estimation accuracy may not be guaranteed; (ii) Under white Gaussian noise scenario, when we form the SCM based Toeplitz matrix, the uniformly distributed noise variance will also be involved in the off-diagonal elements of the Toeplitz matrix. In other words, the white Gaussian noise will be changed to colored noise; (iii) It is assumed in [4–9,28] and [26] that the source number is known *a priori*. However, accurate source number detection remains a challenge. To overcome these drawbacks, we propose a new DOA estimation algorithm that exploits the full information of the  $(2M+1)(M+1)$  fourth-order cumulant matrices, which can work properly even when the source number is not available.

### 3.3. DOA estimation

For notation simplicity, let  $\tilde{\mathbf{C}}_m$  be  $\tilde{\mathbf{C}}_{k_1, k_2, m}$  and  $\phi_{m,i}$  be  $\phi_{k_1, k_2, m}(i)$ . Then  $\tilde{\mathbf{C}}_m$  can be written as

$$\tilde{\mathbf{C}}_m = \tilde{\mathbf{A}} \tilde{\Phi}_m \tilde{\mathbf{A}}^H = \sum_{i=1}^P \phi_{m,i} \tilde{\mathbf{a}}(\theta_i) \tilde{\mathbf{a}}^H(\theta_i). \quad (18)$$

It is obvious that (18) has the joint diagonalization structure and spans the same range space of  $\tilde{\mathbf{A}}$ , i.e.,

$$\text{span}\{\tilde{\mathbf{C}}_m\} = \text{span}\{\tilde{\mathbf{A}}\}. \quad (19)$$

By exploiting the fact that the  $-m$  and  $m$  rows of  $\mathbf{C}_{k_1, k_2}$  are conjugate symmetric, given by  $\mathbf{C}_{k_1, k_2}(-m, \cdot) = \mathbf{C}_{k_1, k_2}^*(m, \cdot)_{M+1}$ . As a result,  $\mathbf{C}_{k_1, k_2}(-m, \cdot)$  and  $\mathbf{C}_{k_1, k_2}(m, \cdot)$  have the same statistical information and there is no need to employ all the  $(2M+1)$  rows to form Toeplitz matrices. Instead, we can choose the first  $(M+1)$  rows of  $\mathbf{C}_{k_1, k_2}$ , and in the sequel there are only  $(M+1)$  Toeplitz matrices containing different statistics. Recalling that  $\tilde{\Phi}_m$  has full rank, we can utilize these  $(M+1)$  Toeplitz matrices to identify the range space of the array manifold matrix  $\tilde{\mathbf{A}}$

and estimate the DOA parameters. For the  $p$ th source, there always exists a vector  $\mathbf{b}_p \in \mathbb{C}^{M+1}$  that is orthogonal to the range space spanned by the remaining  $(P-1)$  steering vectors except  $\tilde{\mathbf{a}}(\theta_p)$ . Hence, we have

$$\mathbf{b}_p \perp \text{range}\{\tilde{\mathbf{a}}(\theta_1), \dots, \tilde{\mathbf{a}}(\theta_{p-1}), \tilde{\mathbf{a}}(\theta_{p+1}), \dots, \tilde{\mathbf{a}}(\theta_P)\}. \quad (20)$$

Equivalently, we obtain

$$\tilde{\mathbf{a}}^H(\theta_i) \mathbf{b}_p = \begin{cases} \tilde{\mathbf{a}}^H(\theta_i) \mathbf{b}_p, & i = p \\ 0, & i \neq p. \end{cases} \quad (21)$$

Substituting (21) into (18) yields

$$\tilde{\mathbf{C}}_m \mathbf{b}_p = \sum_{i=1}^P \phi_{m,i} \tilde{\mathbf{a}}(\theta_i) \tilde{\mathbf{a}}^H(\theta_i) \mathbf{b}_p = g_m \tilde{\mathbf{a}}(\theta_p) \quad (22)$$

where  $g_m = \phi_{m,p} \tilde{\mathbf{a}}^H(\theta_p) \mathbf{b}_p$ . From (22), we confirm that if  $\theta$  is one of the true DOAs, there always exists a scalar  $g_m$  that makes  $\tilde{\mathbf{C}}_m \mathbf{b}$  and  $\tilde{\mathbf{a}}(\theta)$  parallel, i.e.,

$$\tilde{\mathbf{C}}_m \mathbf{b} = g_m \tilde{\mathbf{a}}(\theta), \quad -M \leq m \leq 0. \quad (23)$$

Since (23) holds true for  $-M \leq m \leq 0$ , we try to minimize the total distance between the  $(M+1)$  equations in (23). This leads to the following optimization problem for finding the azimuth  $\theta$  [24,31]

$$\begin{aligned} \min_{\theta} \quad & \mathbf{J}(\theta, \mathbf{g}, \mathbf{b}) = \sum_{m=-M}^0 \|\tilde{\mathbf{C}}_m \mathbf{b} - g_m \tilde{\mathbf{a}}(\theta)\|^2 \\ \text{s.t.} \quad & \|\mathbf{g}\| = 1 \end{aligned} \quad (24)$$

where  $\tilde{\mathbf{a}}(\theta)$  is the steering vector characterized by the parameter of interest  $\theta$ ,  $\mathbf{b}$  is a  $(M+1) \times 1$  vector and  $\mathbf{g} = [g_{-M}, \dots, g_0]$ . For a given  $\theta$ , both  $\mathbf{b}$  and  $\mathbf{g}$  are functions of  $\theta$ . Note that the constraint  $\|\mathbf{g}\| = 1$  is used to avoid the trivial solution of (24), i.e.,  $\mathbf{g} = \mathbf{b} = \mathbf{0}$ .

Since  $\mathbf{b}$  and  $g_m$  are unknown parameters, it is difficult to solve (24) by searching the DOAs directly. To circumvent this issue, we simplify (24) such that the optimization does not depend on  $\mathbf{b}$  and  $g_m$ . To this end, we follow [24] to expand the cost function (24) as

$$\begin{aligned} \mathbf{J}(\theta, \mathbf{g}, \mathbf{b}) &= \mathbf{b}^H \left( \sum_{m=-M}^0 \tilde{\mathbf{C}}_m^H \tilde{\mathbf{C}}_m \right) \mathbf{b} \\ &\quad - \mathbf{b}^H \left( \sum_{m=-M}^0 g_m \tilde{\mathbf{C}}_m^H \tilde{\mathbf{a}}(\theta) \right) \\ &\quad - \left( \sum_{m=-M}^0 g_m^* \tilde{\mathbf{a}}^H(\theta) \tilde{\mathbf{C}}_m \right) \mathbf{b} \\ &\quad + \tilde{\mathbf{a}}^H(\theta) \tilde{\mathbf{a}}(\theta) \sum_{m=-M}^0 |g_m|^2. \end{aligned} \quad (25)$$

Let

$$\mathbf{F} = \sum_{m=-M}^0 \tilde{\mathbf{C}}_m^H \tilde{\mathbf{C}}_m \in \mathbb{C}^{(M+1) \times (M+1)} \quad (26)$$

$$\mathbf{G}(\theta) = [\tilde{\mathbf{C}}_{-M}^H \tilde{\mathbf{a}}(\theta), \dots, \tilde{\mathbf{C}}_0^H \tilde{\mathbf{a}}(\theta)] \in \mathbb{C}^{(M+1) \times (M+1)}. \quad (27)$$

Recalling that  $\tilde{\mathbf{a}}^H(\theta) \tilde{\mathbf{a}}(\theta) = M+1$  and  $\|\mathbf{g}\|^2 = \sum_{m=-M}^0 |g_m|^2$ , (25) can be rewritten as

$$\mathbf{J}(\theta, \mathbf{g}, \mathbf{b}) = \mathbf{b}^H \mathbf{F} \mathbf{b} - \mathbf{b}^H \mathbf{G}(\theta) \mathbf{g} - \mathbf{g}^H \mathbf{G}^H(\theta) \mathbf{b} + (M+1) \|\mathbf{g}\|^2. \quad (28)$$

By using the method of Lagrange multiplier, we have

$$\mathbf{L}(\theta, \mathbf{g}, \mathbf{b}) = \mathbf{J}(\theta, \mathbf{g}, \mathbf{b}) + \varrho \cdot (\|\mathbf{g}\|^2 - 1). \quad (29)$$

**Table 1**

Pseudo-code of proposed algorithm.

---

Step 1: Use (9) to calculate  $(2M+1)(M+1)$  fourth-order cumulant matrices of  $\mathbf{x}(t)$ , i.e.,  $\mathbf{C}_{ij}$ ,  $-M \leq i \leq j \leq M$ .

Step 2: For each cumulant matrix, choose its first  $(M+1)$  rows and each row is utilized to form  $(M+1)$  Toeplitz matrices in (18), i.e.,  $\{\tilde{\mathbf{C}}\}_{m=-M}^0$ .

Step 3: Use (26) and (27) to construct the matrices  $\mathbf{F}$  and  $\mathbf{G}(\theta)$ , respectively.

Step 4: Utilize (40) to form the pseudo-spectrum  $P(\theta)$ .

Step 5: Estimate the DOAs by searching for the peaks of  $P(\theta)$ .

---

For fixed  $\theta$  and  $\mathbf{g}$ , similar to [24] and [31] taking the first-order gradient with respect to  $\mathbf{b}$  yields

$$\frac{\partial \mathbf{L}(\theta, \mathbf{g}, \mathbf{b})}{\partial \mathbf{b}} = \frac{\partial \mathbf{J}(\theta, \mathbf{g}, \mathbf{b})}{\partial \mathbf{b}} = 2(\mathbf{F}\mathbf{b} - \mathbf{G}(\theta)\mathbf{g}) = 0 \quad (30)$$

which leads to

$$\mathbf{b}_{\text{opt}} = \mathbf{F}^\dagger \mathbf{G}(\theta)\mathbf{g}. \quad (31)$$

Substituting (31) into (28), the optimization problem is reduced to

$$\min_{\theta} \mathbf{J}(\theta, \mathbf{g}) = M+1 - \mathbf{g}^H \mathbf{G}^H(\theta) \mathbf{F}^\dagger \mathbf{G}(\theta) \mathbf{g}. \quad (32)$$

Minimizing (32) equals to maximizing  $\mathbf{g}^H \mathbf{G}^H(\theta) \mathbf{F}^\dagger \mathbf{G}(\theta) \mathbf{g}$ . Let  $\sum_{i=1}^{M+1} \lambda_i \mathbf{u}_i \mathbf{u}_i^H$  be the eigenvalue decomposition of  $\mathbf{G}^H(\theta) \mathbf{F}^\dagger \mathbf{G}(\theta)$  with  $\lambda_1 \geq \dots \geq \lambda_{M+1}$  being the eigenvalues and  $\{\mathbf{u}_1, \dots, \mathbf{u}_{M+1}\}$  being the corresponding eigenvectors. Let  $\mathbf{g}$  be a linear combination of the eigenvectors of  $\mathbf{G}^H(\theta) \mathbf{F}^\dagger \mathbf{G}(\theta)$ , i.e.,

$$\mathbf{g} = \nu_1 \mathbf{u}_1 + \dots + \nu_T \mathbf{u}_T \quad (33)$$

where  $T \leq M+1$ . Substituting (33) into  $\mathbf{g}^H \mathbf{G}^H(\theta) \mathbf{F}^\dagger \mathbf{G}(\theta) \mathbf{g}$  yields

$$\begin{aligned} \mathbf{g}^H \mathbf{G}^H(\theta) \mathbf{F}^\dagger \mathbf{G}(\theta) \mathbf{g} &= \mathbf{g}^H \sum_{i=1}^{M+1} \lambda_i \mathbf{u}_i \mathbf{u}_i^H \mathbf{g} \\ &= \nu_1^2 \lambda_1 + \dots + \nu_T^2 \lambda_T. \end{aligned} \quad (34)$$

Since  $\lambda_1$  is the maximum eigenvalue of  $\mathbf{G}^H(\theta) \mathbf{F}^\dagger \mathbf{G}(\theta)$ , (34) can be rewritten as

$$\mathbf{g}^H \mathbf{G}^H(\theta) \mathbf{F}^\dagger \mathbf{G}(\theta) \mathbf{g} \leq (\nu_1^2 + \dots + \nu_T^2) \lambda_1. \quad (35)$$

It follows  $\|\mathbf{g}\|^2 = 1$  that

$$\nu_1^2 + \dots + \nu_T^2 = 1. \quad (36)$$

Substituting (36) into (35), the maximum of  $\mathbf{g}^H \mathbf{G}^H(\theta) \mathbf{F}^\dagger \mathbf{G}(\theta) \mathbf{g}$  becomes

$$\max_{\theta} \mathbf{g}^H \mathbf{G}^H(\theta) \mathbf{F}^\dagger \mathbf{G}(\theta) \mathbf{g} = \lambda_1 \quad (37)$$

where the equation holds true if and only if  $\mathbf{g} = \mathbf{u}_1$ . Therefore, (32) can be further simplified as

$$\min_{\theta} \mathbf{J}(\theta) = M+1 - \max \text{eig}\{\mathbf{G}^H(\theta) \mathbf{F}^\dagger \mathbf{G}(\theta)\} \quad (38)$$

where  $\max \text{eig}(\cdot)$  represents the maximum eigenvalue of a matrix.

There are total  $(2M+1)(M+1)$  cumulant matrices containing different statistical information and each cumulant matrix can form  $(M+1)$  Toeplitz matrices. Note that all the Toeplitz matrices have the same diagonalization structure.

Hence, the cost function can be rewritten as

$$\min_{\theta} \mathbf{J}(\theta) = \sum_{i=1}^{(2M+1)(M+1)} M+1 - \max \text{eig}\{\mathbf{G}^H(\theta) \mathbf{F}^\dagger \mathbf{G}(\theta)\}. \quad (39)$$

Therefore, the pseudo output power spectrum for coherent signals becomes

$$P(\theta) = \frac{1}{(2M+1)(M+1)^2 - \sum_{i=1}^{(2M+1)(M+1)} \max \text{eig}\{\mathbf{G}^H(\theta) \mathbf{F}^\dagger \mathbf{G}(\theta)\}}. \quad (40)$$

The complete procedure of the proposed method is summarized in Table 1.

**Remark 2.** Recalling that the number of rows of  $\tilde{\mathbf{C}}_m$  in (14), namely,  $(M+1)$ , must be larger than or equal to  $P$ . Unlike the forward only spatial smoothing (FOSS) [16], forward-backward spatial smoothing (FBSS) [18] and ESPRIT-like [28] algorithms, our solution does not depend on the source number. Therefore, it is much more attractive for practical applications. Due to this advantage, the proposed algorithm is able to resolve up to  $(M+1)$  sources with  $(2M+1)$  sensors. However, the ESPRIT-like algorithm can only handle at most  $M$  sources.

**Remark 3.** Note that in Section 3.3, the idea has been used in [24,29–31]. The methods in [24,29,30] are designed only for uncorrelated signals. Although the approach in [31] is able to deal with coherent signals, its performance will degrade in spatially correlated noise scenario since it is designed under white Gaussian noise assumption. Unlike the conventional subspace based methods [26–28], the proposed method does not need the knowledge of source number. In particular, it follows from (40) that the source number and the DOAs are selected as the number of highest local maxima of  $P(\theta)$  and the corresponding angles, respectively.

#### 4. Simulation results

In this section, we examine the behavior of the proposed technique. We consider a ULA of  $N=5$  omnidirectional sensors with half-wavelength spacing. The SNR is defined as the ratio of the power of all source signals to that of the additive noise at each sensor. In the following examples, we assume that the sources are 4QAM signals and noise is spatially correlated Gaussian distributed. The  $(k,l)$  element of the noise covariance matrix is given by

$$\mathbf{R}_n(k, l) = \sigma_n^2 \gamma^{|k-l|} e^{j\pi(k-l)/2} \quad (41)$$

where the power level  $\sigma_n^2$  is adjusted to give the desired SNR and  $\gamma$  is a regression coefficient which is used to adjust the spatial correlation between noise. Here, a larger  $\gamma$  corresponds a larger correlation and  $\gamma=0$  means the noise is white Gaussian process. Note that this noise model has been used in [19,20].

In the first example, we consider three sources with one coming from  $\theta_1 = 21^\circ$  and a group of two coherent sources coming from  $\theta_2 = -30^\circ$  and  $\theta_3 = -10^\circ$ . The number of snapshots is  $L=500$  and the SNR is set to be 8 dB. We consider two cases:  $\gamma=0.7$  and  $\gamma=0$ , i.e., spatially correlated Gaussian noise and white Gaussian noise. The performances of the proposed and FBSS algorithms are compared. Meanwhile, we also introduce a fourth-order cumulant (FOC) based method [24] that does not need the source number information for comparison. For the FBSS method, the subarray size is 4. Fig. 2(a) displays the normalized spatial spectra, where the normalization is performed by subtracting the smallest value of output power and then dividing the maximum value of the spectrum. The true DOAs are plotted with black dash lines. We can see from the curves that the proposed algorithm correctly resolves all the sources under the spatially correlated noise scenario. However, the FOC method has only one successful peak of  $\theta_1$  but fails to resolve the other two coherent signals. This is because the FOC scheme is

not able to deal with coherent signals. Although the FBSS method succeeds to generate three visible peaks, there is a large deviation between the estimated and true DOAs. This deviation is mainly caused by the spatially correlated Gaussian noise. Fig. 2(b) is plotted under white Gaussian noise case. It is seen that the FBSS method has a smaller bias compared to Fig. 2(a) and it achieves the best angle resolution. The proposed method also resolves the three DOAs correctly, whereas the FOC method only has two peaks and it fails to estimate the two coherent DOAs.

In the second test, we compare the proposed method with the FBSS, ESPRIT-like [28], FOC and EVESPA [26] algorithms in terms of root mean square error (RMSE). We assume that for the FBSS, ESPRIT-like and EVESPA algorithms, the number of sources is known. We consider three sources with one coming from  $\theta_1 = 20^\circ$  and a group of two coherent sources coming from  $\theta_2 = -42^\circ$  and  $\theta_3 = -15^\circ$ . The number of snapshots is  $L=800$ . We now consider a more severe noise scenario, where a larger  $\gamma$  is used, i.e.,  $\gamma=0.9$ . We set  $\sigma_n^2 = 1$  and vary the signal power such that the input SNR increases from  $-5$  dB to 30 dB. For the FBSS method, the subarray size is 4. 1000 Monte Carlo simulations have been carried out to evaluate the RMSE, which is defined as

$$RMSE = \sqrt{\frac{1}{1000P} \sum_{i=1}^P \sum_{j=1}^{1000} (\hat{\theta}_{ij} - \theta_i)^2}. \quad (42)$$

It is observed from Fig. 3(a) that the proposed method achieves the best estimation performance at low SNRs. The ESPRIT-like and FOC algorithms cannot work properly under the spatially correlated noise and coherent signal case. The EVESPA outperforms the FBSS method but it fails to achieve a performance improvement as the SNR increases. We observe that the proposed estimator outperforms the FBSS method when  $SNR < 15$  dB while the opposite occurs in high SNR region. This is because the aperture of the FBSS is larger than that of the proposed scheme. Moreover, at high SNRs, the spatially correlated noise has little perturbation and larger effective aperture is more important. When SNR is larger than 20 dB, the FBSS method outperforms the proposed one and achieves the best performance. Fig. 3(b) shows the empirical probability of resolution versus SNR. Here, the probability of resolution is calculated by introducing a binary hypothesis. Let  $\Theta = [\theta_1 - \delta, \theta_1 + \delta] \cup \dots \cup [\theta_p - \delta, \theta_p + \delta]$  be the hypothesis, where  $\delta$  is the RMSE corresponding to the threshold SNR and  $[\theta_p - \delta, \theta_p + \delta]$  is the  $p$ th DOA sector. If all the DOA estimates are successfully localized in their own sectors, we say all the DOAs are successfully estimated. For example, after 1000 independent tests, assuming that there are  $N_s$  times that all the DOAs are successfully estimated, the probability of resolution is calculated as  $N_s/1000$ . In this example,  $\delta$  is selected to be  $0.7^\circ$ . It is seen that the proposed scheme has the largest probability of resolution. The proposed and FBSS methods have a full probability of resolution when  $SNR > 15$  dB. However, the EVESPA fails to attain the probability of one. Moreover, it follows from Fig. 3(a) that its RMSE does not decrease as SNR becomes larger.

Let us now study the RMSE performance as a function of sample size. We fix the SNR at 10 dB and vary the number of snapshots from 100 to 1000. The other

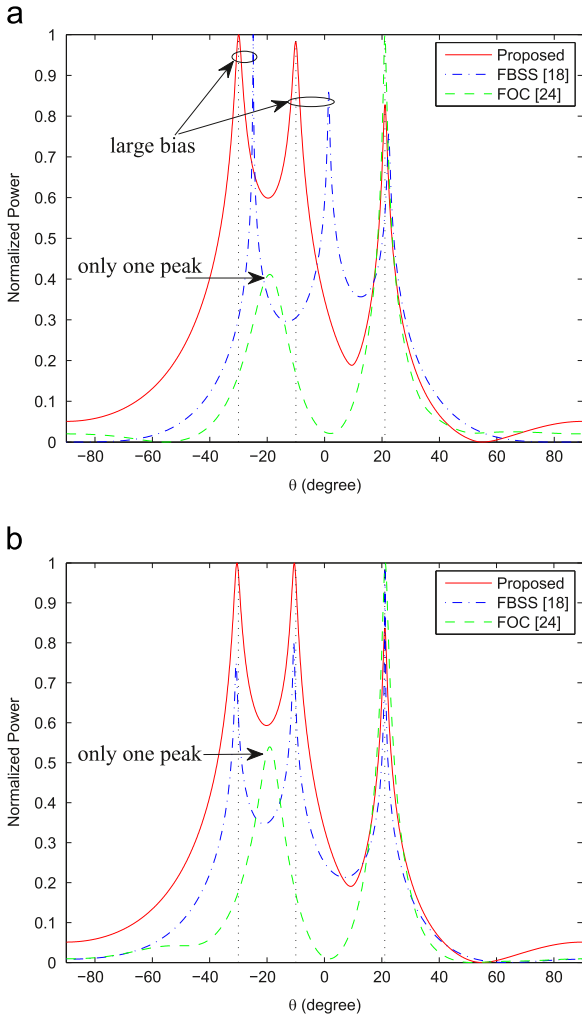
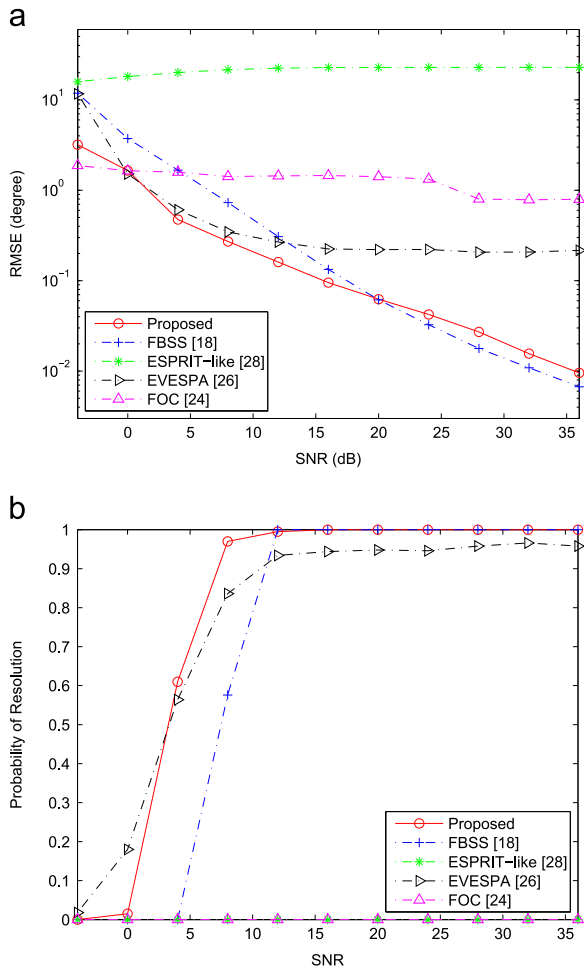


Fig. 2.  $N=5$ ,  $L=500$ ,  $SNR=8$  dB, one source from  $21^\circ$  and a group of coherent sources from  $-30^\circ$  and  $-10^\circ$ . (a) Colored noise with  $\gamma=0.7$  and (b) white noise with  $\gamma=0$ .



**Fig. 3.** RMSE performance versus SNR. ( $N=5$ ,  $L=800$ ,  $\gamma=0.9$ , one source from  $20^\circ$  and a group of coherent sources from  $-42^\circ$  and  $-15^\circ$ .) (a) RMSE versus SNR and (b) probability of resolution versus SNR.

parameters are the same as the second experiment. Fig. 4 (a) shows the RMSEs. We also plot the probability of resolution in Fig. 4(b). It is seen from Fig. 4(a) that the proposed scheme achieves the best performance, followed by the EVESPA. However, the ESPRIT-like method still performs the worst because it uses only a small part of information contained in the covariance matrix and fails to eliminate the impact of the severe noise. For the FOC scheme, it is robust to the spatially correlated noise, but it still performs poorly due to the fact that it cannot deal with coherent signals.

Next, we consider a case when there are three sources from  $\theta_1 = -10^\circ$ ,  $\theta_2 = 8^\circ$  and  $\theta_3 = 35^\circ$ , whereas SNR and the number of snapshots are fixed at 12 dB and  $L=800$ . Note that the first source is uncorrelated with the other two sources. In Fig. 5(a), the RMSEs of the estimated DOAs are plotted as a function of the correlation coefficient  $\rho$  between the second and the third sources. Here, the correlated source samples are generated from a first-order autoregressive process:

$$s_3(i) = \rho s_2(i) + \sqrt{1 - |\rho|^2} \cdot e(i), \quad i = 1, \dots, N. \quad (43)$$

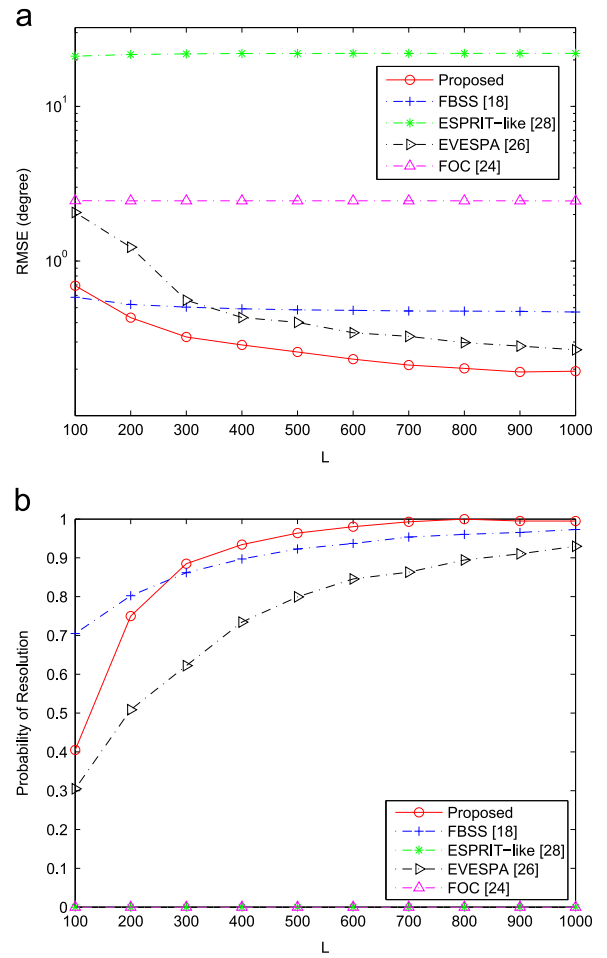


**Fig. 4.** RMSE performance versus sample size. ( $N=5$ , SNR=10 dB,  $\gamma=0.9$ , one source from  $20^\circ$  and a group of coherent sources from  $-42^\circ$  and  $-15^\circ$ .) (a) RMSE versus  $L$  and (b) probability of resolution versus  $L$ .

It can be seen that the performances of the proposed and FBSS methods are independent of the correlation between the two sources, whereas the performance of the FOC method deteriorates as  $\rho$  increases. Compared to the other four estimators, the proposed scheme achieves a considerable improvement in accuracy, no matter the signals are correlated or uncorrelated. Fig. 5(b) shows the probability of resolution as a function of correlation coefficient. It is seen that when the signals are uncorrelated or partially correlated, the proposed and FBSS methods can resolve all the DOAs. However, when the signals are highly correlated or even coherent, the FBSS fails to resolve almost 50% DOAs, whereas the proposed approach can still have a resolution probability of 100%.

## 5. Conclusion

A novel direction finding algorithm based on the joint diagonalization structure of a set of Toeplitz matrices is devised for coherent signals in the presence of spatially correlated noise. The decorrelation of coherent signals is realized via matrix Toeplitz method. By using the

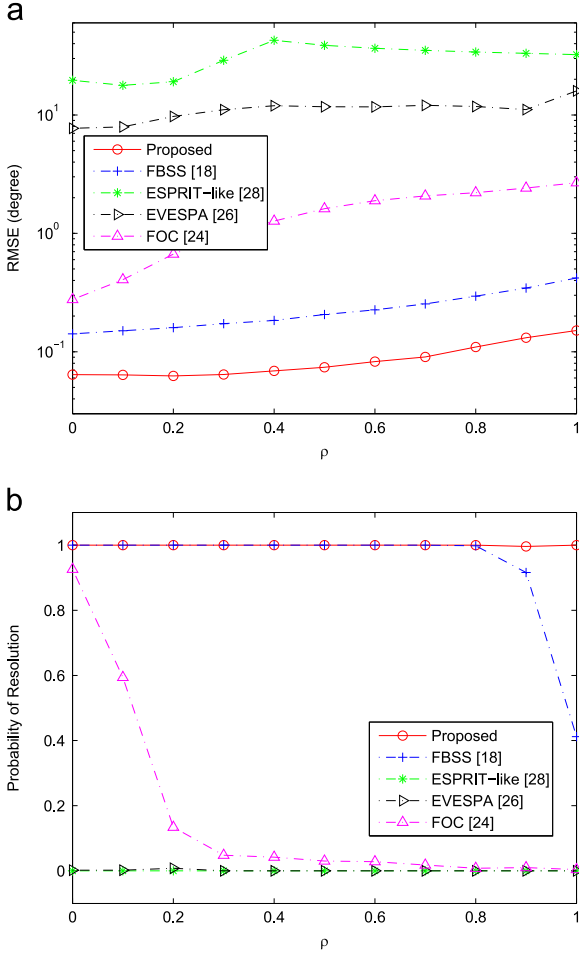


Fig. 5. RMSE performance versus correlation coefficient. ( $N=5$ , SNR=10 dB,  $\gamma=0.9$ , one source from  $-10^\circ$  and a group of correlated sources from  $8^\circ$  and  $35^\circ$ ). (a) RMSE versus  $\rho$  and (b) probability of resolution versus  $\rho$ .

fourth-order cumulant technique, the proposed algorithm can construct  $(2M+1)(M+1)^2$  Toeplitz matrices provided that a ULA of  $(2M+1)$  elements is adopted. The most favorable advantage of the proposed scheme is that it does not require to know the number of sources. Such an advantage is highly desirable for practical applications since accurate detection of source number is still a challenging problem. Simulation results demonstrate the effectiveness of the proposed algorithm.

#### Appendix A. Proof of Proposition 1

Before proving, let us introduce some properties of cumulant that are used in the following derivation [25]:

**CP1:** If  $\{\alpha_i\}_{i=1}^n$  are constants and  $\{x_i\}_{i=1}^n$  are random variables, then

$$\text{cum}(\alpha_1 x_1, \dots, \alpha_n x_n) = \left( \prod_{i=1}^n \alpha_i \right) \text{cum}(x_1, \dots, x_n). \quad (\text{A.1})$$

**CP2:** Cumulant is additive

$$\text{cum}(x_1 + y_1, x_2, \dots, x_n)$$

$$= \text{cum}(x_1, \dots, x_n) + \text{cum}(y_1, \dots, y_n). \quad (\text{A.2})$$

**CP3:** If the random variables  $\{x_i\}_{i=1}^n$  are independent of the random variables  $\{y_i\}_{i=1}^n$ , then

$$\text{cum}(x_1 + y_1, \dots, x_n + y_n) = \text{cum}(x_1, \dots, x_n) + \text{cum}(y_1, \dots, y_n). \quad (\text{A.3})$$

The derivation starts with the estimation of a  $(N \times N)$  fourth-order cumulant matrix  $\mathbf{C}_{k_1, k_2}(l_1, l_2)$  with the  $(k, l)$  element being

$$\begin{aligned} \mathbf{C}_{k_1, k_2}(l_1, l_2) &= \text{cum}(x_{k_1}, x_{k_2}^*, x_{l_1}, x_{l_2}^*) \\ &= \text{cum} \left( \sum_{p=1}^P a_{k_1 p} s_p(t), \sum_{q=1}^P a_{k_2 q}^* s_q^*(t), \right. \\ &\quad \left. \sum_{m=1}^P a_{l_1 m} s_m(t), \sum_{n=1}^P a_{l_2 n}^* s_n^*(t) \right) \\ &+ \text{cum}(n_{k_1}(t), n_{k_2}^*(t), n_{l_1}(t), n_{l_2}^*(t)) \\ &= \text{cum} \left( s_1(t) \sum_{p=1}^K a_{k_1 p} \beta_p + \sum_{p=K+1}^P a_{k_1 p} s_p(t), \right. \\ &\quad \left. s_1^*(t) \sum_{q=1}^K a_{k_2 q}^* \beta_q^* + \sum_{q=K+1}^P a_{k_2 q}^* s_q^*(t), \right. \\ &\quad \left. s_1(t) \sum_{m=1}^K a_{l_1 m} \beta_m + \sum_{m=K+1}^P a_{l_1 m} s_m(t), \right. \\ &\quad \left. s_1^*(t) \sum_{n=1}^K a_{l_2 n}^* \beta_n^* + \sum_{n=K+1}^P a_{l_2 n}^* s_n^*(t) \right) \\ &= \text{cum} \left( s_1(t) \sum_{p=1}^K a_{k_1 p} \beta_p, s_1^*(t) \sum_{q=1}^K a_{k_2 q}^* \beta_q^*, \right. \\ &\quad \left. s_1(t) \sum_{m=1}^K a_{l_1 m} \beta_m, s_1^*(t) \sum_{n=1}^K a_{l_2 n}^* \beta_n^* \right) \\ &+ \text{cum} \left( \sum_{p=K+1}^P a_{k_1 p} s_p(t), \sum_{q=K+1}^P a_{k_2 q}^* s_q^*(t), \right. \\ &\quad \left. \sum_{m=K+1}^P a_{l_1 m} s_m(t), \sum_{n=K+1}^P a_{l_2 n}^* s_n^*(t) \right) \\ &= \sum_{p=1}^K \sum_{q=1}^K \sum_{m=1}^K \sum_{n=1}^K \text{cum}(s_1(t), s_1^*(t), s_1(t), s_1^*(t)) \\ &\quad \cdot a_{k_1 p} a_{k_2 q}^* a_{l_1 m} a_{l_2 n}^* \beta_p \beta_q^* \beta_m \beta_n^* \\ &+ \sum_{p=K+1}^P \sum_{q=K+1}^P \sum_{m=K+1}^P \sum_{n=K+1}^P \\ &\quad \text{cum}(s_p(t), s_q^*(t), s_m(t), s_n^*(t)) \\ &\quad \cdot a_{k_1 p} a_{k_2 q}^* a_{l_1 m} a_{l_2 n}^* \beta_p \beta_q^* \beta_m \beta_n^* \\ &= \sum_{n=1}^K \left( \beta_n^* \gamma_{4, s_1} \sum_{p=1}^K \sum_{q=1}^K \sum_{m=1}^K a_{k_1 p} a_{k_2 q}^* a_{l_1 m} \cdot \beta_p \beta_q^* \beta_m \right) a_{l_2 n}^* \\ &+ \sum_{n=K+1}^P (\gamma_{4, s_n} \cdot |\beta_n|^4 a_{k_1 n} a_{k_2 n}^* a_{l_1 n}) a_{l_2 n}^*. \end{aligned}$$

Define the following intermediate variable

$$\phi_{k_1, k_2, l_1}(n) = \begin{cases} \beta_n^* \gamma_{4, s_1} \sum_{p=1}^K \sum_{q=1}^K \sum_{m=1}^K a_{k_1 p} a_{k_2 q}^* a_{l_1 m} \beta_p \beta_q^* \beta_m, & n = 1, \dots, K \\ \gamma_{4, s_n} \cdot |\beta_n|^4 a_{k_1 n} a_{k_2 n}^* a_{l_1 n}, & n = K+1, \dots, P \end{cases}$$

Then, for  $-M \leq l_1, l_2 \leq M$ , we have

$$\mathbf{C}_{k_1, k_2}(l_1, l_2) = \sum_{n=1}^P a_{l_2 n}^* \phi_{k_1, k_2, l_1}(n)$$

$$= \sum_{n=1}^P \phi_{k_1, k_2, l_1}(n) \cdot e^{j2\pi l_2 \sin \theta_n / d}. \quad (\text{A.5})$$

This completes the proof of Proposition 1.  $\square$

## References

- [1] I. Bekkerman, J. Tabrikian, Target detection and localization using MIMO radars and sonars, *IEEE Trans. Signal Process.* 54 (10) (2006) 3873–3883.
- [2] K.T. Wong, M.D. Zoltowski, Closed-form underwater acoustic direction-finding with arbitrarily spaced vector hydrophones at unknown locations, *IEEE J. Oceanic Eng.* 22 (3) (1997) 566–575.
- [3] X. Sheng, Y.H. Hu, Maximum likelihood multiple-source localization using acoustic energy measurements with wireless sensor networks, *IEEE Trans. Signal Process.* 53 (1) (2005) 44–53.
- [4] R.H. Roy, T. Kailath, ESPRIT-estimation of parameters via rotational invariance techniques, *IEEE Trans. Acoust. Speech Signal Process.* 37 (7) (1989) 984–995.
- [5] C. Qian, L. Huang, H.C. So, Computationally efficient ESPRIT for DOA estimation using the Nyström method, *Signal Process.* 94 (1) (2014) 74–80.
- [6] M. Haardt, A.N. Josef, Unitary ESPRIT: How to obtain increased estimation accuracy with a reduced computational burden, *IEEE Trans. Signal Process.* 43 (5) (1995) 1232–1242.
- [7] R. Schmidt, Multiple emitter location and signal parameter estimation, *IEEE Trans. Antennas Propag.* 34 (3) (1986) 276–280.
- [8] C. Qian, L. Huang, H.C. So, Improved unitary root-MUSIC for DOA estimation based on pseudo-noise resampling, *IEEE Signal Process. Lett.* 21 (2) (2014) 140–144.
- [9] X. Mestre, M.Á. Lagunas, Modified subspace algorithms for DOA estimation with large arrays, *IEEE Trans. Signal Process.* 56 (2) (2008) 598–614.
- [10] M. Wax, K. Thomas, Detection of signals by information theoretic criteria, *IEEE Trans. Acoust. Speech Signal Process.* 33 (2) (1985) 387–392.
- [11] Q.T. Zhang, K.M. Wong, P.C. Yip, J.P. Reilly, Statistical analysis of the performance of information theoretic criteria in the detection of the number of signals in array processing, *IEEE Trans. Acoust. Speech Signal Process.* 37 (10) (1989) 1557–1567.
- [12] M. Wax, T. Kailath, Detection of signals by information theoretic criteria, *IEEE Trans. Acoust. Speech Signal Process.* 33 (2) (1985) 387–392.
- [13] M. Wax, Detection and localization of multiple sources in noise with unknown covariance, *IEEE Trans. Signal Process.* 40 (1) (1992) 245–249.
- [14] E. Fishler, H.V. Poor, Estimation of the number of sources in unbalanced arrays via information theoretic criteria, *IEEE Trans. Signal Process.* 53 (9) (2005) 3543–3553.
- [15] L. Huang, S. Wu, X. Li, Reduced-rank MDL method for source enumeration in high-resolution array processing, *IEEE Trans. Signal Process.* 55 (12) (2007) 5658–5667.
- [16] T.J. Shan, M. Wax, T. Kailath, On spatial smoothing for direction-of-arrival estimation of coherent signals, *IEEE Trans. Acoust. Speech Signal Process.* 33 (4) (1985) 806–811.
- [17] C. Qi, Y. Wang, Y. Zhang, Y. Han, Spatial difference smoothing for DOA estimation of coherent signals, *IEEE Signal Process. Lett.* 12 (11) (2005) 800–802.
- [18] S.U. Pillai, B.H. Kwon, Forward/Backward spatial smoothing techniques for coherent signal identification, *IEEE Trans. Acoust. Speech Signal Process.* 37 (1) (1989) 8–15.
- [19] M. Viberg, P. Stoica, B. Ottersten, Maximum likelihood array processing in spatially correlated noise fields using parameterized signals, *IEEE Trans. Signal Process.* 45 (4) (1997).
- [20] K.M. Wong, J.P. Reilly, Q. Wu, S. Qiao, Estimation of the directions of arrival of signals in unknown correlated noise—Part I: the MAP approach and its implementation, *IEEE Trans. Signal Process.* 40 (8) (1992) 2007–2028.
- [21] K. Werner, M. Jansson, DOA estimation and detection in colored noise using additional noise-only data, *IEEE Trans. Signal Process.* 55 (11) (2007) 5309–5322.
- [22] J.P. Le Cadre, Parametric methods for spatial signal processing in the presence of unknown colored noise fields, *IEEE Trans. Signal Process.* 37 (7) (1989) 965–983.
- [23] S.A. Vorobyov, A.B. Gershman, K.M. Wong, Maximum likelihood direction-of-arrival estimation in unknown noise fields using sparse sensor arrays, *IEEE Trans. Signal Process.* 53 (1) (2005) 34–43.
- [24] W.-J. Zeng, X.L. Li, X.D. Zhang, Direction-of-arrival estimation based on the joint diagonalization structure of multiple fourth-order cumulant matrices, *IEEE Signal Process. Lett.* 16 (3) (2009) 164–167.
- [25] M.C. Doğan, J.M. Mendel, Applications of cumulants to array processing—Part I: aperture extension and array calibration, *IEEE Trans. Signal Process.* 43 (5) (1995) 1200–1216.
- [26] E. Gonen, J.M. Mendel, M.C. Dogan, Applications of cumulants to array processing—Part IV: direction finding in coherent signals case, *IEEE Trans. Signal Process.* 45 (9) (1997) 2265–2276.
- [27] B. Porat, B. Friedlander, Direction finding algorithms based on high-order statistics, *IEEE Trans. Signal Process.* 39 (9) (1991) 2016–2024.
- [28] F.M. Han, X.D. Zhang, An ESPRIT-like algorithm for coherent DOA estimation, *IEEE Antennas Wirel. Propag. Lett.* 4 (2005) 443–446.
- [29] W.-J. Zeng, X.L. Li, High-resolution multiple wideband and nonstationary source localization with unknown number of sources, *IEEE Trans. Signal Process.* 58 (6) (2010) 3125–3136.
- [30] W.-J. Zeng, X.L. Li, H.C. So, Direction-of-arrival estimation based on spatial-temporal statistics without knowing the source number, *Signal Process.* 93 (12) (2013) 3479–3486.
- [31] C. Qian, L. Huang, W.-J. Zeng, H.C. So, Direction-of-arrival estimation for coherent signals without knowledge of source number, *IEEE Sensors Journal* 14 (9) (2014) 3267–3273.